

dc transport studies of poly(benzimidazobenzophenanthroline) a ladder-type polymer

K. S. Narayan* and A. A. Alagiriswamy

Chemistry and Physics of Materials Unit, Jawaharlal Nehru Centre For Advanced Scientific Research, Jakkur, Bangalore-560064, India

R. J. Spry

Wright Laboratory, Materials Directorate, Wright Patterson Air Force Base, Dayton, Ohio 45434

(Received 17 November 1997; revised manuscript received 26 May 1998)

The room-temperature electrical conductivity of poly(benzimidazobenzophenanthroline) dramatically increases when heated to 600 K by more than six orders in magnitude. The evolution of this significant increase in conductivity is studied closely. The conductivity prior to exposure to the high temperature is compared with postheated samples and analyzed in terms of activated and hopping models. The thermally induced electrical conductivity is studied for different geometries and significant anisotropic features are observed. The variation in the thermally induced conductivity with respect to the ambient conditions is also correlated with the structure. The results reveal contribution of surface processes in the electronic transport.

[S0163-1829(99)06015-4]

I. INTRODUCTION

The rigid-rod and aromatic heterocyclic ladder-type polymers have been characterized extensively for their mechanical properties, and they promise multifunctional purposes compared to the linearly conjugated polymers because of their extensive π electron delocalization, coupled with high mechanical strength, and thermal stability.^{1,2} It has been suggested that the existence of multiple conjugation paths would also result in higher conductivity because the charge carriers could bypass the defects on one of the chains.³ However, there are far fewer studies on the electronic transport of these rigid-rod and ladder-type polymers compared to the conventional conducting polymers such as polyacetylene, polyaniline, polypyrrole, etc.⁴ Another aspect that has not been studied in conventional conducting polymers, primarily due to lack of thermal stability, is the behavior of electronic properties in the high-temperature (500–700 K) regime and investigation of shallow traps.

The fully conjugated ladder polymer poly(benzimidazobenzophenanthroline) (BBL) provides a model system because of its stability at temperatures up to 600 °C in air and 700 °C in nitrogen and the processability by which thin films and fibers of micron-size diameter can be obtained.^{1,2} These polymers, in the form of films or fibers, due to their high molecular weight, display good mechanical properties (high tensile strength, high modulus) and exceptional solvent chemical resistance and high intrinsic viscosity (8.9 dl/gm).^{1,2,5} The polymer has a repeat unit that possesses a double-stranded chemical structure consisting of aromatic naphthalenic and benzenoid units and alternating bond lengths of imines in the neutral ground state. Recently wide angle x-ray measurements of BBL films have revealed scattering patterns suggesting that molecular chains are arranged in a layered configuration with their molecular planes almost perpendicular to the film surface.⁶ It is expected that the ladder-like BBL polymer chains form a layered structure across the film thickness like other stiff polymers. The high degree of coplanarity is reflected in the anisotropy of conductivity even

for samples with film thickness ranging up to 15 μm with the in-plane conductivity greater than three orders of magnitude than the out of plane conductivity.^{7,8} The absorption spectrum shows the onset of π - π^* transition at around 1.68 eV with a broad absorption maxima at about 1.9 eV.⁹ The broad transition spanning over a range of 0.22 eV was attributed to the wide distribution of length scales of the conjugated system and other broadening mechanisms arising from the disorder in the system. The photocurrent studies also revealed the band edge observed in the absorption spectra but show subtle differences with respect to the photon energy when the measurements are carried in the surface and sandwich configurations.⁹

It is also been observed that dc conductivity in pristine BBL films depends on ambient conditions and varies from 10^{-11} to 10^{-14} S/cm.¹⁰ Some of the methods to enhance the conductivity in BBL have been through chemical doping,¹¹ ion implantation,¹² pressure treatment,¹³ pyrolysis,¹⁴ and heat treatment.^{2,8} Humidity-dependent studies reveal surface effects which dominate the transport process.¹⁰ However, the thermally induced processes are more pronounced with conductivity changing by nearly seven orders in magnitude at room temperature when heated to 625 K. In this paper we study the thermally induced electronic conductivity closely and speculate on the mechanism leading to this enhancement. The temperature dependence of the conductivity and the stability of the electronic properties depend on the sample history and morphological aspects. Polymer samples in film and fiber forms are studied to resolve these unique features. The anisotropy in conductivity and the dependence on ambient conditions of the enhanced conductivity are also studied.

II. EXPERIMENT

The cast films of 20 μm thickness and oriented fibers of 15 μm in diameter were used for the present studies. Films were obtained from the polymer solution with methane sulfonic acid as the solvent. The dc conductivity of the films as

well as fibers were measured by the standard four-probe and two-probe methods. The conductivity cell consists of four electrodes with a spring loaded arrangement specially designed for reliable high-temperature measurements under high vacuum. The contact regions on the samples were coated with gold for uniformity and measurements for resistance were done in the Ohmic region from the current-voltage curves. The temperature was monitored by the suitable thermocouples and platinum sensors along with a digital Keithley multimeter (model 2001) and current was measured using a Keithley 6512 electrometer. The measurements were carried out for a wide range of temperature as possible with the sample resistance of $10^{12} \Omega$ as the limit of measurements.

III. RESULTS AND DISCUSSION

The room-temperature conductivity of the BBL as measured by four-probe conductivity of cast films with equidistant electrodes on the plane of the film, $\sigma_{\parallel} \cong 10^{-8} \text{ S/cm}$. The conductivity perpendicular to the film, $\sigma_{\perp} \cong 10^{-12} \text{ S/cm}$, and that of the fiber, with the electrodes placed along the fiber axis, $\sigma_{\text{fib}} \cong 5 \times 10^{-7} \text{ S/cm}$. The values of the conductivity in different configurations reveal the anisotropy present in cast films. The source of anisotropy could arise from extrinsic effects leading to modification of surface states or can be intrinsic in origin. The importance of these extrinsic effects can be studied by the temperature dependence of the anisotropy. The conductivity σ of the film and fiber in different configurations as a function of temperature, T is shown in Fig. 1. Fig. 1(a) shows that the plot of $\sigma_{\perp}(T)$ and the arrow traces the thermal cycle in the measurement process. The predominant features accompanying the cycle of measurement is the presence of large hysteresis in $\sigma(T)$ between the initial heating process and the subsequent cooling and warming process. There was no discernible hysteresis in $\sigma_{\perp}(T)$ upon repeated heating and cooling after the initial first round. However, if the sample is heated in the first round to a T_{max} lower than 600 K, appreciable hysteresis is obtained for $\sigma_{\perp}(T)$ during the subsequent cooling and warming cycles. The $T_{\text{max}} \sim 625 \text{ K}$, the temperature corresponding to a minimum in the area of the hysteresis between the first round cooling and second round heating, can be assigned to the maximum value of an energy barrier which is thermally accessible for increasing the conductivity. Preliminary thermally stimulated current measurements also reveal peaks indicative of well-defined trap energy levels.

The conductivity measurement of the sample with the probes along the surface, i.e., $\sigma_{\parallel}(T)$ showed similar behavior to that shown in Fig. 1(b). However, the subtle differences become more obvious in the anisotropy $\sigma_{\parallel}/\sigma_{\perp}$ as a function of temperature. The anisotropy profile as a function of temperature is shown in Fig. 2(b) and shows a broad maximum centered around 430 K. $\sigma_{\perp}(T)$ increases more rapidly than $\sigma_{\parallel}(T)$ for $T > 430 \text{ K}$ and the ratio $\sigma_{\parallel}/\sigma_{\perp}$ settles down to 400 as the temperature is increased. The ratio is fairly independent of temperature subsequently on cooling and reheating. The anisotropy decreases by three orders in magnitude after the thermal treatment at room temperature.

Measurements done on fiber also qualitatively reveal similar $\sigma_{\text{fib}}(T)$ behavior as depicted in Fig. 1(c). The magnitudes of the conductivity, however, are shifted by three to

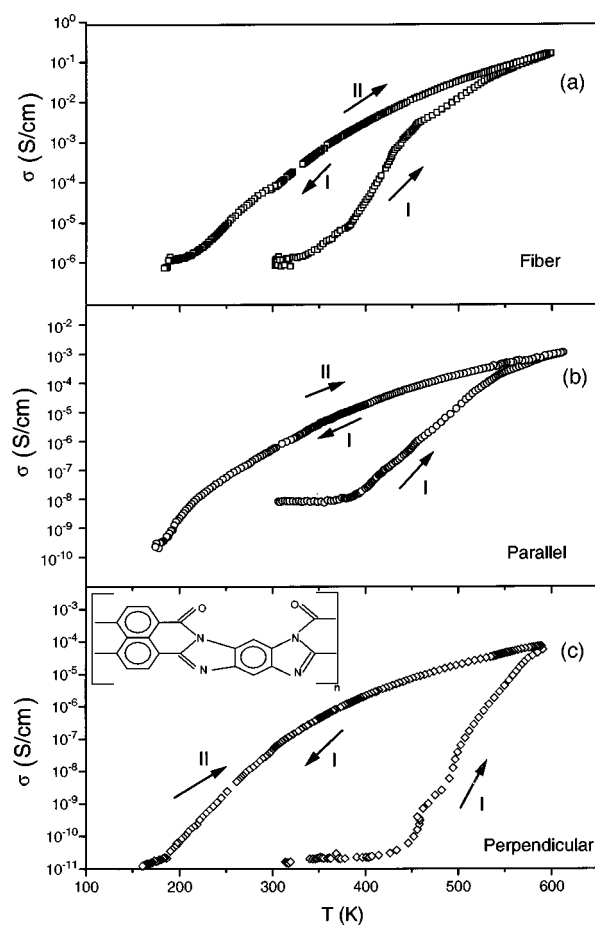


FIG. 1. $\sigma(T)$ as a function of temperature for fiber (a), parallel (b), and perpendicular (c) configurations. The arrow indicates the thermal cycle, *I* indicates first round of heating and cooling, and *II* indicates second round of heating and cooling. The chemical structure of BBL is also depicted in the inset.

four orders in magnitude with $\sigma_{\text{fib}}(T) \cong 1 \text{ S/cm}$ at $T = 600 \text{ K}$. The high conductivity value is expected due to an increased degree of crystallinity, order and chain orientation. The anisotropy profile as a function of temperature is shown in Fig. 2(a). The $\sigma_{\text{fib}}(T)/\sigma_{\perp}(T)$ shows a broad maximum centered around 430 K. $\sigma_{\perp}(T)$ increases more rapidly than $\sigma_{\text{fib}}(T)$ for $T > 430 \text{ K}$ and the ratios settle down to 3500 as the temperature is increased.

The conductivity mechanism changes prior to sample getting exposed to $T \sim 600 \text{ K}$ and thereafter as evidenced from Figs. 1 and 3. The mechanism crossover can also be benchmarked in terms of the temperature dependence of the anisotropy. As the sample is heated the crossover temperature can correspond to the point where the anisotropy ratio $\sigma_{\text{fib}}(T)/\sigma_{\perp}(T)$ decreases to a constant value of ~ 3500 and is nearly temperature independent.

The anisotropy present prior to heating can be considered to arise from extrinsic ambient sources which preferentially modifies the surface compared to the bulk and gives rise to the peculiar temperature dependence with a rounded maximum around 430 K. The anisotropy after the sample is heated to 625 K and maintained in vacuum conditions can correspond to some sort of intrinsic anisotropy of the system as indicated by the lack of temperature dependence.

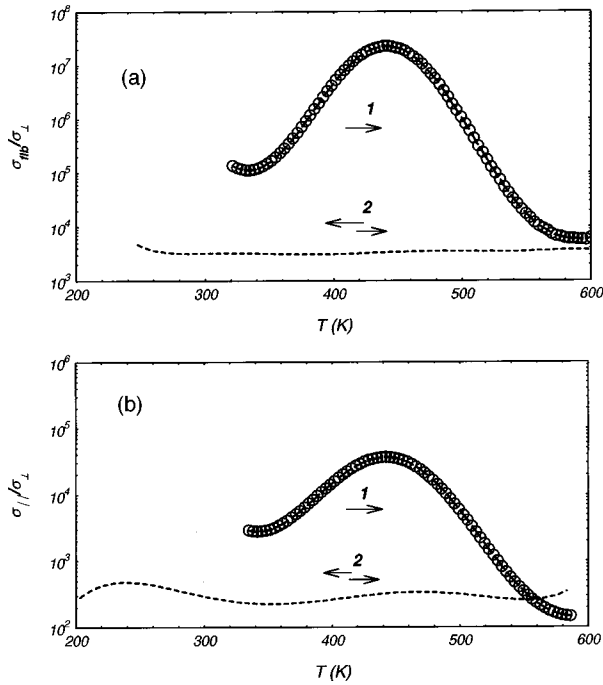


FIG. 2. Anisotropy in conductivity as a function of temperature for the entire thermal cycle (a) $(\sigma_{\text{fib}}/\sigma_{\perp})$ vs T , (b) $(\sigma_{\parallel}/\sigma_{\perp})$ vs T ; the arrow indicates the thermal cycle, 1 indicates first round of heating, and 2 indicates second round of heating and cooling.

The time dependence of conductivity mentioned above also supports the view of different mechanisms for the charge transport process. The conductivity value for all the systems at room temperature, in vacuum conditions after heating, is fairly constant; however, the value gradually drops over a period of hours when exposed to air and converges to its original value as shown in Fig. 4. Earlier reports on the humidity dependence of BBL were explained on the basis of H_2O adsorption where the sites close to the surface are significantly affected.¹⁰ The samples studied were, however, in the highly insulating regime. The fiber conductivity was more stable with respect to ambient conditions. The high conductivity of the fiber at room temperature obtained by heating persisted longer. These results suggest that the fiber is less sensitive to moisture indicating that the diffusion rates are small when compared to films and they have not altered the electronic properties. Also thermogravimetric analysis (TGA) studies indicate there is a marginal weight loss below the degradation temperature of BBL at 675 K, which can be attributed due to the moisture content in the samples.

The difference in the energetics of the mechanisms can be gauged by fits to the simple activated models. The fits are not crude as expected and the barrier energies obtained can be used to highlight the differences. The initial heating process of the three configurations can be modeled in terms of an activated behavior and conductivity via barrier hopping as the leading mechanism. There is a gradual increase in $\sigma_{\perp}(T)$ up to 440 K, which can be approximately fitted to a simple activated model: $\sigma = \sigma_0 \exp(-\Delta/kT)$ with $\Delta \approx 0.0452$ eV. $\sigma_{\perp}(T)$ increases more rapidly for $T > 440$ K and is indicated in the fit to the activated model with the value of Δ of ≈ 2.308 eV. $\sigma_{\perp}(T)$ for $T = 600$ K is in the order of 10^{-5} S/cm. For the surface measurement, $\sigma_{\parallel}(T)$ of BBL

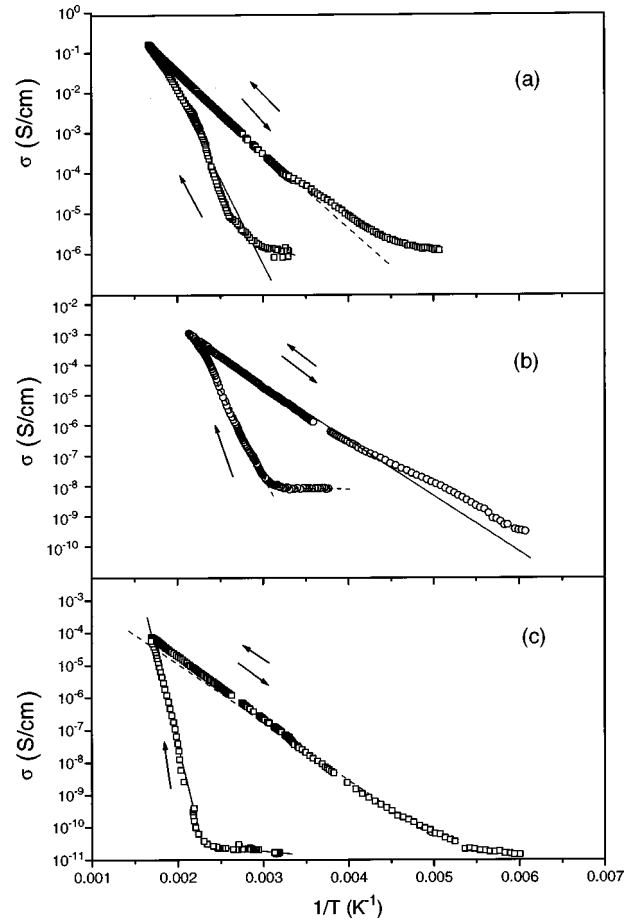


FIG. 3. $\sigma(T)$ for the entire thermal cycle in log scale as a function of reciprocal of temperature for different configurations fiber (a), parallel (b), and perpendicular (c), respectively, and the arrow indicates the thermal cycle. The dashed and solid lines indicate fits to a simple activation behavior model.

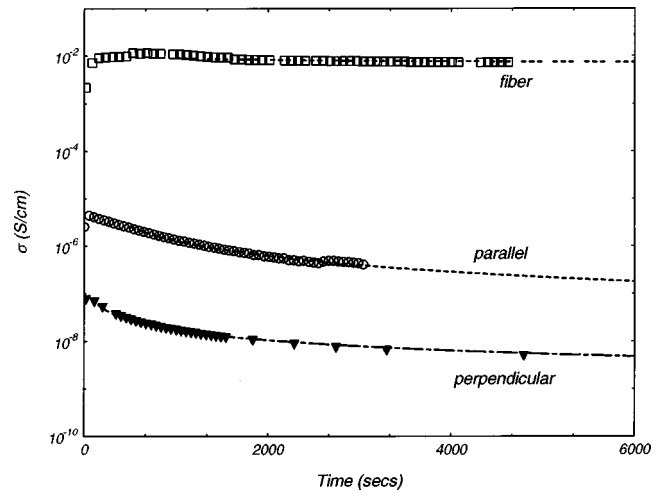


FIG. 4. $\sigma(t)$ as a function of time for heated samples at room temperature and exposed to air for different configurations. $t = 0$ sec corresponds to vacuum conditions, and dashed lines are fits to the data.

films, the initial heating process can be modeled in terms of a simple activated behavior with two different regimes; $\Delta \cong 0.011$ eV for $T < 390$ K and $\Delta \cong 1.12$ eV for $600 > T > 390$ K, and $\sigma \cong 10^{-3}$ S/cm at $T = 600$ K. For the fiber measurement, $\sigma_{\text{fib}}(T)$, the initial heating process can also be modeled in terms of a simple activated behavior with two different regimes; $\Delta \cong 0.098$ eV for $T < 350$ K and $\Delta \cong 0.878$ eV for $600 > T > 350$ K, and $\sigma_{\text{fib}} \cong 0.1$ S/cm at $T = 600$ K.

Upon cooling from 600 K, $\sigma(T)$ for the different film geometries and fiber can also be approximately fitted to a single activated process. $\sigma_{\perp}(T)$ gradually decreases uniformly on cooling with $\Delta \cong 0.35$ eV and reaches $\cong 10^{-8}$ S/cm at room temperature. $\sigma_{\parallel}(T)$ gradually decreases uniformly on cooling with $\Delta \cong 0.364$ eV reaching $\cong 10^{-6}$ S/cm at room temperature. $\sigma_{\text{fib}}(T)$ gradually decreases uniformly on cooling with $\Delta \cong 0.377$ eV approaching $\cong 10^{-4}$ S/cm at room temperature. The notable feature is that the activation energy values for all configurations and fibers are almost similar.

The results obtained after the initial heating process ($T_{\text{max}} \cong 625$ K) can be considered to be a better representative of the system for studying the electronic transport process because of the insensitivity to subsequent heating cycles yielding consistent results. Three-dimensional (3D) Mott variable range hopping (VRH) models have been previously used to describe the $\sigma(T)$ behavior with $\sigma(T) = \sigma_0 \exp(T_0/T)^{\gamma}$ where $(1/\gamma - 1)$ is the dimensionality and for isotropic system $\sigma_{\parallel} = \sigma_{\perp}$, the parameter $T_0 = A/k_B N_D(E_F) \varepsilon^D$ where ε is the localization length, N_D is the density of localized states near the fermi level in D dimensions and A is a numerical factor of order unity.¹⁵ For anisotropic 3D system the effective ε is equivalent to a geometrically averaged $(\varepsilon_{\parallel}^2 \varepsilon_{\perp})^{1/3}$ where ε_{\parallel} and ε_{\perp} are intraplane and interplane localization lengths. The conductivity anisotropy, i.e., $\sigma_{\parallel}/\sigma_{\perp}$ in the model¹⁶ is found to be $\sim (\varepsilon_{\parallel}/\varepsilon_{\perp})^2$. The ratio of the localization lengths $(\varepsilon_{\parallel}/\varepsilon_{\perp})$ for BBL have been estimated to be ~ 30 .⁷ The present value of $\sigma_{\parallel}/\sigma_{\perp} \sim 400$, which is in the same order of magnitude as $(\varepsilon_{\parallel}/\varepsilon_{\perp})^2$ can be then argued to arise from the anisotropy in localization length. However, in the present case $\sigma_{\parallel}(T)$, $\sigma_{\perp}(T)$, and $\sigma_{\text{fib}}(T)$ yields better fits to quasi-1D models than 2D, 3D VRH, or a simple activated model. The deviation from a 3D model, which was used to describe the transport properties in BBL,⁷ can be attributed to differences in factors such as orientation, impurity concentration, and processing conditions. The low-dimensional picture is more plausible for the micron-size, drawn fibers, which can be considered to be packed with fibrillar structures as observed in scanning electron microscopy images and these structures are present in the films as well.

Another crucial feature in the present case is lack of temperature dependence of $\sigma_{\parallel}/\sigma_{\perp}$ for surface and bulk configurations and $\sigma_{\parallel}/\sigma_{\perp}$ for fiber and bulk configurations. This feature is also revealed in the similar values of T_0 obtained in the 1D model fits (Fig. 5), with values of $T_0 \sim 2.23 \times 10^5$, 2.31×10^5 , and 2.37×10^5 K, for bulk, surface, and fiber configurations respectively. The system can be modeled in terms of a quasi-1D system with a strong intrachain hopping and a weak interchain hopping component. For the

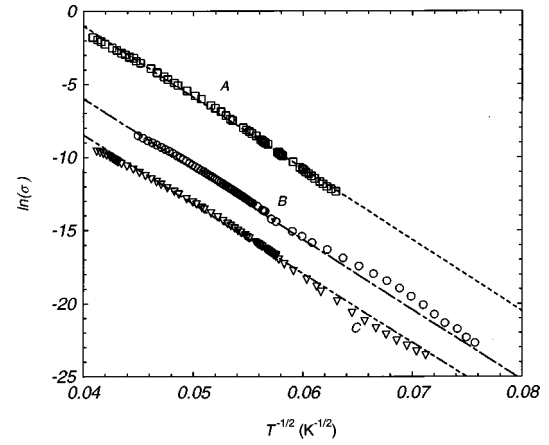


FIG. 5. $\ln(\sigma)$ vs $1/\sqrt{T}$ for the heated samples fiber (a), parallel (b), and perpendicular (c) configurations. The dashed lines are fits to the 1D variable range hopping model.

component of interchain hopping conductivity parallel to the chain, $\sigma_{\parallel}(T) = \{[e^2 v_{\text{ph}} (2\pi t_{\perp} \tau_i h)^2] / (\alpha K_B T z A)\} \exp[-(T_0/T)^{1/2}]$ and the component of interchain hopping perpendicular to the chain, $\sigma_{\text{inter}}(T) = \{[2e^2 g(E_F) b^2 v_{\text{ph}}] / A (2\pi t_{\perp} \tau_i h)^2\} \exp[-(T_0/T)^{1/2}]$, where $T_0 = 8\alpha / (g(E_F) z k_B)$, v_{ph} is the characteristic phonon frequency, t_{\perp} is the interchain exchange integral, τ_i is the interchain mean free time, α is the inverse of longitudinal localization length, b is the inverse of transverse localization length, z is the number of nearest neighboring chains, A is the average cross-sectional area of each chain, and $g(E_F)$ is the density of states with one sign of spin.^{17,18} A detailed structural information on the arrangement of the polymer chains in the bulk is needed to know how the quasi-1D models can be adopted for $\sigma_{\perp}(T)$. However, it must be mentioned that several other models also result in this kind of temperature dependence such as charge energy limited tunneling for granular metal and 3D variable range hopping model with a Coulomb gap.¹⁸ It is not possible with the present experimental information to have a complete understanding of the physical process involved in the conduction mechanism, but, what is established is the identical nature of the temperature dependence of the conductivity in different geometries and morphology after thermal treatment.

The x-ray studies done on uniaxially oriented films revealed Bragg peaks at $\theta \sim 13.24^\circ$ and 19.01° with d values corresponding to 3.36 and 2.36 Å, respectively, and are consistent with the earlier observations.⁶ Preliminary observations in the x-ray studies also reveal additional features which are dependent on the sample history. Fibers are expected to show a microstructure similar to the uniaxially grown films. Efforts are being pursued to study these features in detail as a function of temperature and correlate the results with the transport results.

The samples when exposed to air vary significantly with respect to time after heat treatments. Upon exposing the sample $\sigma_{\parallel}(t)$ and $\sigma_{\text{fib}}(t)$ initially increases marginally and subsequently ($t > 100$ sec) the conductivity in all configurations progressively decreases with time as shown in Fig. 4. The decrease in $\sigma(t)$ can be fitted to $\ln(\sigma) = at^b$ where a and b are constants. The rate of decrease in conductivity for the different geometries can be evaluated in terms of magnitude

of the constant b , since $d\sigma/dt = b\sigma \ln(\sigma)/t$. The fiber conductivity decreases at a much slower rate compared to $\sigma_{\parallel}(t)$ and $\sigma_{\perp}(t)$ with $b \sim 0.04$, 0.08 , and 0.02 for bulk, surface, and fiber configurations, respectively. This process is irreversible and the sample regains the higher conductivity ($t=0$ value) only upon thermal treatment. These features indicate the sensitivity of the electronic properties on the physiochemical interactions at the surface. The results also clearly demonstrate that these changes brought about extrinsically can be overcome by thermal treatment.

Earlier studies on the pressure dependence of the electronic transport of the thermally treated polymer in ambient conditions also show the anisotropic behavior.¹³ The resistance in the transverse configuration R_{tr} and in the planar surface configuration R_{sur} show drastically different behavior as a function of pressure. The R_{tr} of the sample gradually decreases with an increasing pressure with the process being reversible. The surface resistance on the other hand increases with increasing pressure initially and then decreases for $P > 25$ kbar with an appearance of a rounded peak at $P \sim 20$ kbar and this process was irreversible. A possible explanation for the results was given in terms of the occurrence of an initial physiochemical process such as removal of water from the surface for $P < 20$ kbar, and subsequently physical processes such as packing, and orientational changes taking over for $P > 25$ kbar as the major factors influencing the dc conductivity.¹³

Previous results on photocurrent studies on heated samples in ambient conditions reveal a small but significant presence of photocurrent in the surface cell configuration, well below the absorption edge (< 1.68 eV).⁹ In contrast to the surface cell configuration photocurrent the sandwich cell

configuration photocurrent follows the absorption spectra closely around the edge.⁹ A possible source for this effect was thought to arise from the presence of extrinsic impurities that can cause tails in the density of states by perturbing the band edge via deformation potential, via coulomb interaction or by forming a band of impurity states. The present results may explain the origin of the features observed in the pressure dependence and photoconductivity results and stress the importance of geometrical effects in the experimental studies due to the surface processes in this material.

IV. CONCLUSION

The present results add further insight into the electronic structure of BBL and the sensitivity of electronic properties to ambient conditions and thermal treatment. The ambiguous manner in which the conductivity of BBL enhances due to thermal treatment and the decrease upon exposure to moisture is completely traced and the results are consistent with previous experimental observations. The energy barriers and the time constants involved in these process are also estimated. The anisotropy in the electronic conductivity studied as a function of these parameters also highlights the importance of structural and morphological aspects in the ladder-type polymer.

ACKNOWLEDGMENTS

K.S.N. acknowledges the support of the Asian Office of Aerospace Research and Development (AOARD), AFOSR, and Department of Science and Technology, Government of India, towards this project.

*Author to whom correspondence should be addressed. Electronic address: narayan@jncasr.ac.in

¹(a) F. E. Arnold and R. L. Van Deusen, *Macromolecules* **2**, 497 (1969); (b) F. E. Arnold and R. L. Van Deusen, *J. Appl. Polym. Sci.* **15**, 2035 (1971).

²(a) S. A. Jenekhe, L. R. dePaor, X. L. Chen, and R. M. Tarkka, *Chem. Mater.* **8**, 2401 (1996); (b) C. S. Wang, C. Y. C. Lee, and F. E. Arnold, in *Electrical, Optical, and Magnetic Properties of Organic Solid State Materials*, edited by L. V. Chiang, A. F. Garito, and D. J. Sandman, No. 247 of MRS Symposia Proceedings (Materials Research Society, Pittsburgh, 1992), p. 747.

³H. Mizes and E. Conwell, *Phys. Rev. B* **44**, 3963 (1991).

⁴J. W. Blatchford and A. J. Epstein, *Am. J. Phys.* **64**, 120 (1996).

⁵(a) R. L. Van Deusen, *J. Polym. Sci., Polym. Lett. Ed.* **4**, 211 (1966); (b) S. A. Jenekhe and S. J. Tibbetts, *J. Polym. Sci., Part B: Polym. Phys.* **26**, 201 (1988); (c) S. A. Jenekhe and P. O. Johnson, *Macromolecules* **23**, 4419 (1990).

⁶H. H. Song, A. V. Fratini, M. Chabiny, G. E. Price, A. K. Agrawal, C. S. Wang, J. Burkette, D. S. Dudis, and F. E. Arnold, *Synth. Met.* **69**, 533 (1995).

⁷F. Coter, Y. Belaish, D. Davidov, L. R. Dalton, E. Ehrenfreund, M. R. Mclean, and H. S. Nalwa, *Synth. Met.* **29**, E471 (1989).

⁸K. S. Narayan, S. M. Long, A. J. Epstein, B. E. Taylor, R. J. Spry, S. J. Bai, and C. S. Wang, *Bull. Am. Phys. Soc.* **38**, 110 (1993).

⁹K. S. Narayan, B. E. Taylor-Hamilton, R. J. Spry, and J. B. Ferguson, *J. Appl. Phys.* **77**, 3938 (1995).

¹⁰H. Antoniadis, M. A. Abkowitz, J. A. Osaheni, S. A. Jenekhe, and M. Stolka, *Chem. Mater.* **6**, 61 (1994).

¹¹(a) O. K. Kim, *J. Polym. Sci., Polym. Lett. Ed.* **29**, 663 (1982); (b) O. K. Kim, *Mol. Cryst. Liq. Cryst.* **105**, 161 (1984).

¹²(a) S. A. Jenekhe and S. J. Tibbetts, *J. Polym. Sci., Polym. Phys. Ed.* **26**, 201 (1988); (b) J. A. Osaheni, S. A. Jenekhe, A. Burns, G. Du, J. Joo, Z. Wang, A. J. Epstein, and C. S. Wang, *Macromolecules* **25**, 5828 (1992).

¹³K. S. Narayan, A. K. Singh, and S. K. Ramasesha, *J. Phys. D* **30**, L16 (1997).

¹⁴I. Belaish, D. Davidov, H. Selig, M. R. Mclean, and L. R. Dalton, *Angew. Chem. Adv. Mater.* **101**, 1601 (1989).

¹⁵N. F. Mott and E. A. Davis, *Electronic Processes in Non-crystalline Materials* (Clarendon, Oxford, 1984).

¹⁶B. I. Shklovskii and A. L. Efros, *Electronic Properties of Doped Semiconductors*, Springer Series in Solid State Sciences vol. 45, edited by M. Cardona, P. Fulde, and H. J. Queisser (Springer-Verlag, Berlin 1984).

¹⁷E. P. Nakhmedov, V. N. Prigodin, and A. N. Samukhin, *Fiz. Tverd. Tela (Leningrad)* **31**, 31 (1989) [*Sov. Phys. Solid State* **31**, 368 (1989)].

¹⁸Z. H. Wang, H. H. S. Javadi, A. Ray, A. G. MacDiarmid, and A. J. Epstein, *Phys. Rev. B* **42**, 5411 (1990); (b) Z. H. Wang, A. Ray, A. G. MacDiarmid, J. M. Ginder, and A. J. Epstein, *ibid.* **43**, 4373 (1991).